XLI CILAMCE
XLI Ibero-Latin American Congress on Computational Methods in Engineering
16-19 November, 2020 FOZ DO IGUAÇU PARANÁ - BRAZIL

Effect of uncertainties and noise on the nonlinear vibrations of a slender beam

Kaio. C. B. Benedetti[1], Paulo B. Gonçalves[1]

[1]*Dept. of Civil and Environmental Engineering, Pontifical Catholic University of Rio de Janeiro*
R. Marquês de São Vicente, 225, Gávea, 22451-900, Rio de Janeiro/RJ, Brazil
kaio.engcivil@aluno.puc-rio.br, paulo@puc-rio.br

Abstract. Uncertainty analysis is fundamental in structural engineering in order to incorporate imprecise information, errors, and limitations into theoretical models. Various techniques have been developed over the years to access the uncertainty, with advances regarding semilinear boundary value problems to correctly represent the probability spaces, namely spectral decomposition and collocation. However, the analysis is continuously improving for initial value problems, and nonlinear problems in general since the methods developed to decompose the probability spaces do not behave well in such cases. When uncertainties are given in spaces of distributions, such as white noise processes, the applicability of those techniques is even more limited, leaving the Monte Carlo sampling strategies as the final and, in various cases, the only choice of analysis. We consider a planar nonlinear beam equation under an additive white noise excitation and imperfections to exemplify these limitations. To obtain the dynamics of such a system, we spatially discretize the problem using the first linear vibration mode and analyze the resulting differential equation by varying the uncertainty parameters. A stochastic differential equation of Itô type is derived to verify the white noise excitation. We demonstrate the global dynamics through the generalized cell mapping, which is used to construct both the Perron-Frobenius and the Koopman operator of the differential equations. This example shows the effects of noise on the resonant solutions of nonlinear dynamic problems, stabilizing the nonresonant solution. Also, the mutual impact of noise with imperfections demonstrates the correlation of parametric uncertainty with random vibrations.

Keywords: Uncertainties, Noise, Stochastic differential equation, Nonlinear vibrations, Generalized cell mapping.

1 Introduction

Slender structures, such as cables, rods, membranes, and shells, can display various phenomena when dynamically excited. They are susceptible to large displacements and rotations, which implies that nonlinear geometric stiffness contributes significatively to the structure's behavior. Therefore, it is necessary to accurately model these nonlinearities to address the dynamics of such structures.

Specifically, Euler-Bernoulli beams have been subjected to various studies. Nayfeh and Pai [1] explain that nonlinear beam theories tend to be highly coupled, making the analysis a problematic process. One such theory is proposed by Crespo da Silva and Glynn [2, 3], which derived a set of coupled nonlinear third-order equations that govern the flexural-flexural-torsional-inextensional motions of slender beams considering both geometric and inertial nonlinearities. Resonance conditions were verified analytically through multiple scales analysis in several works. For example, Crespo da Silva and Glynn [3] addressed the forced nonplanar motions, Crespo da Silva and Zaretzky [4, 5] studied primary and secondary flexural-torsional resonance and Nayfeh and Arafat [6, 7] obtained the responses to parametric excitation. Later, the dynamic stability under different load conditions and cross-section geometries was investigated by Carvalho, Gonçalves, Rega and Del Prado [8, 9]. The exact Euler-Bernoulli theory is presented by Nayfeh and Pai [1], where they show how simplifications lead to different sets of equations.

Regarding imperfect beams, two analytic approaches can be considered, varying the reference axis. For small imperfections, Aghababaei, Nahvi, Ziaei-Rad [10, 11] showed that a set of perfect axes leads to more straightforward derivations, while Nayfeh and Pai [1] demonstrated that the full curved inertial axes need to be

considered for larger imperfections. However, the small imperfections case needs clarification, with no studies addressing their effect on nonlinear dynamics, except for few resonant cases. Besides parametric uncertainty, the modeling of loads as stochastic processes has been fulfilled by Silva and Gonçalves [12], effectivelly considering a wide frequency spectrum and its action over global dynamics. The same stochastic load was considered by Orlando, Gonçalves, Rega and Lenci [13], observing its effect over the global dynamics of a multistable system.

In the present work the slender beam equation of motion is obtained based on the works by Crespo da Silva and Glynn [2, 3]. The introduction of geometric imperfections is based on the work of Aghababaei, Nahvi, and Ziaei-Rad [10]. However, we consider a case with only flexural motions, simplifying the equations of motion. The effects of additive noise and modal imperfections on the global dynamics are shown with the generalized cell-mapping proposed by Hsu and Chiu [14, 15]. Because of the strong nonlinearities and the probability space of white noise processes being a space of distributions, the Monte Carlo method is employed in the construction of the transfer operators. Precisely, the noise and imperfection effects over nonresonant and resonant solutions are considered, changing the probability measures and basins of attraction.

2 Mathematical formulation

The flexural Euler-Bernoulli beam equation with imperfections is formulated through the extended Hamilton's principle. An elastic material is considered with small elastic strains. After the first modal equation is presented, the transfer operators are addressed.

2.1 Flexural third-order Euler-Bernoulli beam

The kinematics of an imperfect beam is defined with respect to three curvilinear coordinate systems: the deformed axes (ξ, ζ), the undeformed axes (ξ_0, ζ_0) and the material axes (X, Z). The deformed and material axes define the Eulerian and Lagrangian frame of reference, respectively, with the latter corresponding to the perfect model. The undeformed axes represent the imperfect model, which corresponds to a stress-free configuration. A schematic of all three frames is given in Fig. 1, with also the undeformed and deformed arc lengths s and $\tilde{s}$, respectively.

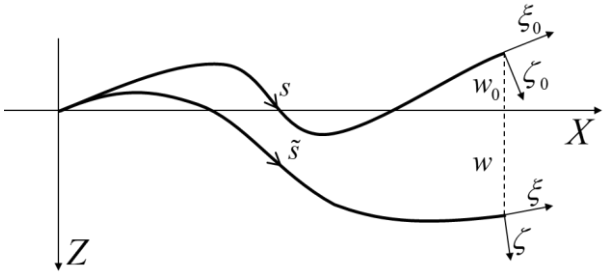

Figure 1 – Orientation of imperfect undeformed and deformed frames with respect to material axes

In the derivation, a damping term c_w and external distributed load Q_w are considered. The nondimensional equation is given by

$$\begin{aligned}\left[\ddot{w}+c_w\dot{w}-Q_w\right]\left(1+\frac{w_0'^2}{2}\right)=\Bigg\{&-\bar{w}'w''\bar{w}''-\frac{1}{2}\left(w_0''w'^2\right)'+w'''\left(\frac{w_0'^2}{2}-1\right)\\&+J_\eta\left[\bar{w}'\dot{w}'^2-\ddot{w}'\left(\frac{w_0'^2}{2}-1\right)\right]+\bar{w}'\left[J_\eta\bar{w}'\ddot{w}'-\bar{w}'w'''-\int_1^x\int_0^x\left(\bar{w}'\dot{w}'\right)^{\bullet}dxdx\right]\Bigg\}',\end{aligned} \tag{1}$$

where $\bar{w}=w+w_0$, $(\,)'=d/dx$, $(\,)^{\bullet}=d/dt$ and J_η is the nondimensional rotational inertia.

A clamped-free beam is considered with the following cantilever boundary conditions

$$\begin{aligned} &w(0,t) = w'(0,t) = 0, \\ &w''(1,t) = w'''(1,t) - J_\eta \ddot{w}'(1,t) = 0. \end{aligned} \tag{2}$$

The displacement field $w(x, t)$ and imperfection $w_0(x)$ are given respectively by

$$w(x,t) = \sum_{i=1}^{\infty} w_i(t)\, {}^iF_w(x), \quad w_0(x) = \sum_{i=1}^{\infty} w_{0i}\, {}^iF_w(x) \tag{3}$$

where ${}^iF_w$ are solutions of the Rayleigh beam equation,

$$\ddot{w} - J_\eta \ddot{w}'' + w^{\mathrm{iv}} = 0, \tag{4}$$

subjected to boundary conditions, eq. (2). Considering the displacement field and imperfection in the form of the first vibration mode, by direct substitution of eq. (3) into eq. (1) followed by a Galerkin projection, the equation of motion of the sdof model is obtained. Assuming a beam with length 20, rectangular cross-section with height 2 and width 1, the equation takes the form

$$\begin{aligned} &\left(1 + 4.5948 w_1^2 + 9.1895 w_1 w_0 + 8.18 w_0^2\right)\ddot{w}_1 + \left(1.0007 + 3.5799 w_0^2\right) c_w \dot{w}_1 \\ &\quad + 4.5948 w_0 \dot{w}_1^2 + \left(12.3147 + 9.9257 w_0^2 + 4.5948 \dot{w}_1^2\right) w_1 \\ &\quad + 90.1911 w_0 w_1^2 + 40.1327 w_1^3 = \left(2.6030 w_0^2 + 0.7832\right) q_w \cos(\Omega t). \end{aligned} \tag{5}$$

Equation (5) is a Duffing type equation with strong nonlinear terms due to the rotational inertia J_η. Also, the imperfection w_0 dictates if second-order terms will be present, which will be demonstrated to change the beam behavior. Rewriting it as a first-order system and considering a standard Brownian motion W_t, eq. (5) becomes

$$\begin{aligned} &\dot{w}_1 = v, \\ &\dot{v} = \Big\{\left(2.6030 w_0^2 + 0.7832\right) q_w \cos(\Omega t) - \left(1.0007 + 3.5799 w_0^2\right) c_w \dot{w}_1 \\ &\qquad - 4.5948 w_0 \dot{w}_1^2 - \left(12.3147 + 9.9257 w_0^2 + 4.5948 \dot{w}_1^2\right) w_1 \\ &\qquad - 90.1911 w_0 w_1^2 - 40.1327 w_1^3 \Big\} \Big/ \left(1 + 4.5948 w_1^2\right. \\ &\qquad \left. + 9.1895 w_1 w_0 + 8.18 w_0^2\right) + \sigma \dot{W}_t \end{aligned} \tag{6}$$

where σ is the standard deviation parameter. This system is formally a Langevin equation, interpreted as a particle within a potential well excited by a deterministic force q_w and a noise fluctuation $\sigma \dot{W}_t$. The derivative of the Brownian motion is formally a white noise. Different interpretations can be considered, such as the Itô and the Stratonovich ones, see Zhang and Karniadakis [16]. The Itô interpretation is here considered, resulting in a stochastic differential equation. Also, the deterministic case is retrieved when $\sigma = 0$.

2.2 Discretization of transfer operators

Equation (6) generates a measurable dynamical system φ_t. The phase-space is the bidimensional euclidean plane, $\mathbb{X} \equiv \mathbb{R}^2$, naturally endowed with the Borel σ-algebra $\mathfrak{B}(\mathbb{X})$, and continuous time $\mathbb{T} \equiv \mathbb{R}$. Differences between the invariant measure structures of the deterministic and stochastic case are substantial since the latter constitutes a cocycle over the random space generated by the random noise. For more details, see L. Arnold [17] and V. Arnold [18].

Despite their differences, the measures' evolution of both deterministic and stochastic dynamical systems are governed by the Perron-Frobenius operator $\mathcal{P}_t$ and the Koopman operator $\mathcal{K}_t$. The Perron-Frobenius operator acts on density distributions f, and is defined as

$$\begin{aligned} &\mathcal{P}_t : L_n(\mathbb{X}) \to L_n(\mathbb{X}), \\ &\int_A \mathcal{P}_t f \, d\mu = \int_{\varphi_t^{-1}(A)} f \, d\mu, \\ &\forall f \geq 0,\ f \in L_n(\mathbb{X}),\ A \in \mathfrak{G}, \end{aligned} \tag{7}$$

where $n \geq 1$. The measure μ can be the Lebesgue measure for deterministic systems or a more complicated structure, such as a Dirac measure or a tensor product between the phase-space and the stochastic space, see Hmissi [19]. Also, the σ-algebra $\mathfrak{G}$ can be $\mathfrak{B}(\mathbb{X})$, for deterministic systems, or $\mathfrak{B}(\mathbb{X}) \times \mathfrak{W}$, with $\mathfrak{W}$ as the σ-algebra of the stochastic space. The Koopman operator is

$$\begin{aligned} &\mathcal{K}_t : L_\infty(\mathbb{X}) \to L_\infty(\mathbb{X}) \\ &\mathcal{K}_t g = g \circ \varphi_t, \\ &\forall g \in L_\infty(\mathbb{X}), \end{aligned} \tag{8}$$

acting on observables g of the dynamical system φ_t. The transfer operators are dual to each other,

$$\langle \mathcal{P}_t f, g \rangle_\mu = \langle f, \mathcal{K}_t g \rangle_\mu . \tag{9}$$

Therefore, one operator can be obtained from the other without further complications.

The Perron-Frobenius operator $\mathcal{P}_t$, in particular, defines a functional linear dynamical system over φ_t. It follows an ensemble of trajectories, where φ_t is the evolution of only one trajectory. Complicated nonlinear flows, both deterministic and stochastic, can be represented in this manner, and each particular topology in φ_t has a counterpart in $\mathcal{P}_t$. For example, Bollt and Santitissadeekorn [20] demonstrated that fixed points are equivalent to atomic measures, $x = \varphi_t x \Leftrightarrow \mathcal{P}_t \delta_x = \delta_x$, and as such, are eigenfunctions with unitary eigenvalues.

The discretization of the transfer operators is considered by the generalized cell-mapping, described by Hsu and Chiu [14, 15]. It is identical to the previously defined Ulam method, see Guder and Kreuzer [21], which approximates $\mathcal{P}_t$ by a zero-order Galerkin method. The phase-space $\mathbb{X}$ is discretized into a disjoint collection of k sets, $\{b_1, \ldots, b_k\}$, and $\mathcal{P}_t$ is approximately given by

$$\mathcal{P}_t \approx p_{ij} = \frac{\mu\left(\varphi_t^{-1}(b_i) \cap b_j\right)}{\mu(b_j)}, \tag{10}$$

where p_{ij} are elements of a stochastic matrix $[p_{ij}]$. These elements correspond to the probability of the system to evolve from set b_j to set b_i under the dynamical system φ_t. Such probabilities are obtained by a Monte Carlo sampling due to the strong nonlinearities of the problem in consideration. Furthermore, the Koopman operator approximation is obtained by the transpose of $[p_{ij}]$, $[k_{ij}] = [p_{ij}]^*$, due to the dual relation in eq. (9).

A significant result is given by Lindner and Hellmann [22]. They showed that the fixed space of $[k_{ij}]$ could be used to approximate the basin structures of φ_t, given that the dynamical system is continuous. This result is explored in this study, and stochastic basins of attractions are obtained by adopting the concept of 0-absorption stability as the infinity time convergence of dynamical systems.

3 Results

3.1 First mode primary resonance

The resonance diagrams for different levels of imperfection are presented in Figure 2, obtained with the continuation of the periodic responses for the deterministic case, $\sigma = 0$. The resonance diagrams are of the hardening-type, with possible nonresonant and resonant solutions for excitation frequencies $\Omega > \omega_{nat}$. As the imperfection increases, the resonance curve shifts toward lower frequencies, changing the frequency band for which the model is susceptible to large amplitude vibrations and amplitude jumps.

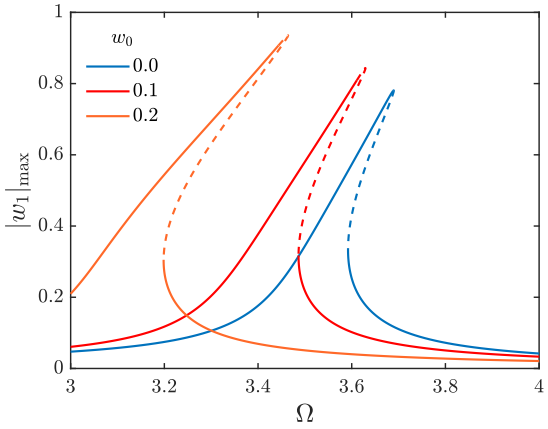

Figure 2 – Resonance curves for increasing geometric imperfection magnitudes and $q_w = 0.2$

3.2 Global dynamics

The global dynamics of eq. (6), for a parameter set where resonant and nonresonant solutions exist, is now addressed. The phase-space window is {-3..3,-9..9}, discretized into 300x900 disjoint sets each with 25x25 initial conditions in the deterministic case, and 5x5 initial conditions in the stochastic case. The boundaries are adopted as absorbing so that solutions that are mapped outside the phase-space are flagged as escape. Specifically, each initial condition is integrated 100 times when the noise term is nonzero. Therefore, 625 and 2500 trajectories are accounted for the deterministic and stochastic case, respectively.

Figure 3 present the results for the deterministic case with $w_0 = 0.05$. The density, Figure 3a, shows the presence of two attracting regions near (0, 0) and (0.5, 2) corresponding to resonant and nonresonant solutions, respectively. The nonresonant densities are more prominent, meaning that more initial conditions in the adopted window converge to these solutions in comparison to the resonant solutions. The basins of attraction of nonresonant and resonant solutions are displayed in Figure 3b, c. Since $\sigma = 0$, the blurred boundaries are the result of the discretization of the transfer operator, eq. (10).

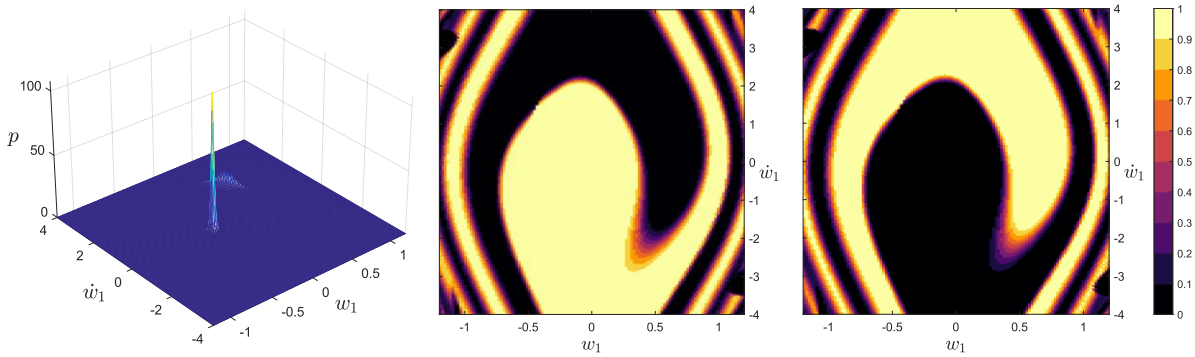

(a) (b) (c)

Figure 3 – Probability density (a), and basins of attraction of nonresonant (b) and resonant (c) solutions for $q_w = 0.2$, $\Omega = 3.632$, $\sigma = 0$, $w_0 = 0$

The stochastic and imperfect case, with $\sigma = 0.05$ and $w_0 = 0.05$, is displayed in Figure 4. The density of the nonresonant region spread out over larger areas in phase-space, decreasing their maximum values, see Figure 4a. The resonant solution also have their areas increased in comparison with the deterministic case. However, this effect is partially nullified by the imperfect case, resulting in lower maximum values for the resonant solution. Stochastic basins of attraction are presented in Figure 4b, c, corresponding to zero escape probability, see Lindner and Hellmann [22]. The noise blurs the basin boundaries so that initial conditions in these regions can converge to

both solutions with a fixed probability. The imperfection also impacts the basin topologies significantly, with the resonant basin not having any region with probability 1. Therefore, solutions can escape to nonresonant solutions in a finite time, with the basins represent a mean expectation of the solutions distribution for $t \to \infty$.

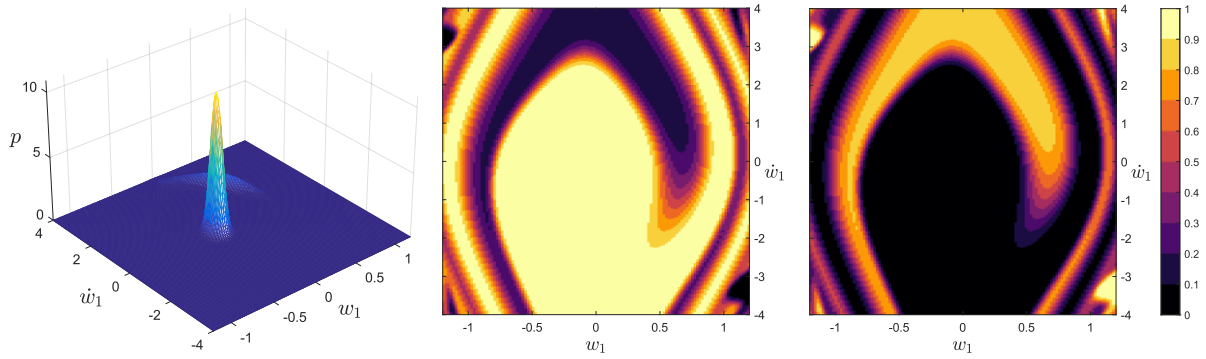

(a) (b) (c)

Figure 4 – Probability density (a), and basins of attraction of nonresonant (b) and resonant (c) solutions for $q_w = 0.2$, $\Omega = 3.632$, $\sigma = 0.05$, $w_0 = 0.05$

4 Conclusions

The effects of modal imperfections and additive noise on the nonlinear and global dynamics of a slender beam are addressed. The resonance curves are obtained for increasing imperfection magnitudes, showing a shift of the curves towards smaller frequencies. The influence of modal imperfections and noise on the global dynamics are studied with the generalized cell-mapping, also named Ulam's method. Modal imperfections destabilize the resonant solutions, agreeing with the result observed in the resonance curves. Furthermore, these solutions are also susceptible to instability due to additive noise, as confirmed by the stochastic basins of attraction: as noise and imperfection increases, the 0-absorption stability region of the resonant solutions shrinks. The detailed basin evolution will be addressed in future research, with different types of noise.

Acknowledgements. The authors acknowledge the financial support of the Brazilian research agencies CAPES [finance code 001], CNPq, FAPERJ-CNE and FAPERJ Nota 10.

Authorship statement. The authors hereby confirm that they are the sole liable persons responsible for the authorship of this work, and that all material that has been herein included as part of the present paper is either the property (and authorship) of the authors, or has the permission of the owners to be included here.

References

[1] A. H. Nayfeh and P. F. Pai, *Linear and Nonlinear Structural Mechanics*. Wiley 2004.
[2] M. R. M. Crespo da Silva and C. C. Glynn, "Nonlinear Flexural-Flexural-Torsional Dynamics of Inextensional Beams. I. Equations of Motion". *J Struct Mech*, vol. 6, n. 4, pp. 437–448, 1978.
[3] M. R. M. Crespo da Silva and C. C. Glynn, "Nonlinear Flexural-Flexural-Torsional Dynamics of Inextensional Beams. II. Forced Motions". *J Struct Mech*, vol. 6, n. 4, pp. 449–461, 1978.
[4] M. R. M. Crespo da Silva and C. L. Zaretzky, "Nonlinear flexural-flexural-torsional interactions in beams including the effect of torsional dynamics. I: Primary Resonance". *Nonlinear Dyn*, vol. 5, n. 1, pp. 3–23, 1994.
[5] C. L. Zaretzky and M. R. M. Crespo da Silva, "Nonlinear flexural-flexural-torsional interactions in beams including the effect of torsional dynamics. II: Combination resonance". *Nonlinear Dyn*, vol. 5, n. 2, pp. 161–180, 1994.
[6] A. H. Nayfeh and H. N. Arafat, "Nonlinear Response of Cantilever Beams to Combination and Subcombination Resonances". *Shock Vib*, vol. 5, n. 5–6, pp. 277–288, 1998.
[7] H. N. Arafat and A. H. Nayfeh, "Nonlinear bending-torsion oscillations of cantilever beams to combination parametric excitations". In: *Proceedings of Society of Photo-Optical Instrumentation Engineers* 1999.
[8] E. C. Carvalho, P. B. Gonçalves, G. Rega, and Z. J. G. N. Del Prado, "Influence of axial loads on the nonplanar vibrations of cantilever beams". *Shock Vib*, vol. 20, n. 6, pp. 1073–1092, 2013.
[9] E. C. Carvalho, P. B. Gonçalves, G. Rega, and Z. J. G. N. Del Prado, "Nonlinear nonplanar vibration of a functionally

graded box beam". *Meccanica*, vol. 49, n. 8, pp. 1795–1819, 2014.
[10] O. Aghababaei, H. Nahvi, and S. Ziaei-Rad, "Non-linear non-planar vibrations of geometrically imperfect inextensional beams, Part I: Equations of motion and experimental validation". *Int J Non Linear Mech*, vol. 44, n. 2, pp. 147–160, 2009.
[11] O. Aghababaei, H. Nahvi, and S. Ziaei-Rad, "Non-linear non-planar vibrations of geometrically imperfect inextensional beams. Part II—Bifurcation analysis under base excitations". *Int J Non Linear Mech*, vol. 44, n. 2, pp. 161–179, 2009.
[12] F. M. A. da Silva and P. B. Gonçalves, "The influence of uncertainties and random noise on the dynamic integrity analysis of a system liable to unstable buckling". *Nonlinear Dyn*, vol. 81, n. 1–2, pp. 707–724, 2015.
[13] D. Orlando, P. B. Gonçalves, G. Rega, and S. Lenci, "Influence of transient escape and added load noise on the dynamic integrity of multistable systems". *Int J Non Linear Mech*, vol. 109, pp. 140–154, 2019.
[14] C. S. Hsu and H. M. Chiu, "A Cell Mapping Method for Nonlinear Deterministic and Stochastic Systems—Part I: The Method of Analysis". *J Appl Mech*, vol. 53, n. 3, pp. 695, 1986.
[15] H. M. Chiu and C. S. Hsu, "A Cell Mapping Method for Nonlinear Deterministic and Stochastic Systems—Part II: Examples of Application". *J Appl Mech*, vol. 53, n. 3, pp. 702, 1986.
[16] Z. Zhang and G. E. Karniadakis, *Numerical Methods for Stochastic Partial Differential Equations with White Noise*. Springer International Publishing, Cham, 2017.
[17] L. Arnold, *Random Dynamical Systems*. Springer Berlin Heidelberg, Berlin, Heidelberg, 1998.
[18] V. I. Arnold, *Mathematical Methods of Classical Mechanics*, 2nd ed. Springer New York, New York, NY, 1989.
[19] M. Hmissi, "On Koopman and Perron-Frobenius operators of random dynamical systems". *ESAIM Proc Surv*, vol. 46, n. November, pp. 132–145, 2014.
[20] E. M. Bollt and N. Santitissadeekorn, *Applied and Computational Measurable Dynamics*. Society for Industrial and Applied Mathematics, Philadelphia, PA, 2013.
[21] R. Guder and E. J. Kreuzer, "Using Generalized Cell Mapping to Approximate Invariant Measures on Compact Manifolds". *Int J Bifurc Chaos*, vol. 07, n. 11, pp. 2487–2499, 1997.
[22] M. Lindner and F. Hellmann, "Stochastic basins of attraction and generalized committor functions". *Phys Rev E*, vol. 100, n. 2, pp. 022124, 2019.